

## THE ORBIT AND COMPANION OF *PROBABLE* $\gamma$ -RAY PULSAR J2339–0533

ROGER W. ROMANI<sup>1</sup> AND MICHAEL S. SHAW  
 Department of Physics, Stanford University, Stanford, CA 94305  
*To Appear in ApJ Letters, 742, L1*

### ABSTRACT

We have measured dramatic flux and spectral variations through the 0.193 d orbit of the optical counterpart of the unidentified  $\gamma$ -ray source 0FGL J2339.8–0530. This compact object companion is strongly heated, with  $T_{eff}$  varying from  $\sim 6900$  K (superior conjunction) to  $< 3000$  K at minimum. A combined fit to the light curve and radial velocity amplitudes implies  $M_1 \approx 0.075M_\odot$ ,  $M_2 \approx 1.4M_\odot$  and inclination  $i \approx 57^\circ$ . Thus this is a likely ‘black widow’ system with a  $\dot{E} \approx 10^{34-34.5} \text{ erg s}^{-1}$  pulsar driving companion mass loss. This wind, also suggested by the X-ray light curve, may prevent radio pulse detection. Our measurements constrain the pulsar’s reflex motion, increasing the possibility of a pulse detection in the  $\gamma$ -ray signal.

*Subject headings:* gamma rays: stars - pulsars: general

### 1. INTRODUCTION

The Large Area Telescope (LAT) on the *Fermi* satellite has revolutionized our understanding of the  $\gamma$ -ray sky, with particular success in detecting spin-powered pulsars and blazars. After only three months of observation, a preliminary 0FGL ‘bright source list’ of 205 objects detected at  $> 10\sigma$  significance was presented in Abdo et al. (2009a). Remarkably, over 95% of these sources now have been associated with lower energy counterparts (Ackerman et al. 2011). Moreover, comparison with the  $\gamma$ -ray properties of the identifications make it possible to classify many of the remaining sources; likely blazars show significant variability, while likely pulsars are steady, but show strongly curved spectra, with cut-offs above a few GeV.

At present, there are two 0FGL sources at  $|b| > 1^\circ$  with pulsar-like properties and no identification. One, 0FGL J2339.8–0530 was a  $\sim 12\sigma$  detection with steady, hard spectrum emission. It has been the subject of both radio pulsar counterpart searches and ‘blind’ searches for  $\gamma$ -ray pulsations (eg. Abdo et al. 2009b). To date no pulsed emission has been seen and the source remains unidentified in the latest catalog (Abdo et al. 2011). There it is listed as 2FGL J2339.6–0532, localized to  $l = 81.357 \pm 0.03$ ,  $b = -62.467 \pm 0.02$ , with a variability index of 15.7 (indicating steady emission) and a flux of  $3.0 \pm 0.2 \times 10^{-11} \text{ erg/cm}^2/\text{s}$ , with a hard  $\Gamma = 1.96$  spectrum showing  $6\sigma$  evidence of a spectral cutoff. It thus remains one of the best unidentified pulsar candidates. Indeed, Kong et al. (2011ab), have drawn attention to this source, finding that there was an optically variable star coincident with a *CXO* source in the LAT uncertainty region, arguing that this was likely a ‘radio-quiet’ millisecond pulsar (MSP) and suggesting that it may be an LMXB in quiescence, similar to the LAT-associated LMXB/MSP transient FIRST J102347.6+003841 (Archibald et al. 2010; Tam et al. 2010). We report here on optical imaging and spectroscopy of this source which support the millisecond pulsar hypothesis, but instead show that this is a ‘black-widow’ type pul-

sar, evaporating a low mass companion, similar to the original of such systems, PSR B1957+20, but  $2-3\times$  closer at  $d \sim 1$  kpc. We suggest that strong outflow in this evaporating system inhibits detection of radio pulsations. If the pulsed emission can be detected in the LAT photons, the resulting orbital information will make this a double-line spectroscopic binary and should allow an unusually precise determination of the neutron star mass, comparable to the important high  $M_{\text{PSR}} = 2.40 \pm 0.12M_\odot$  determination recently made for PSR B1957+20 (van Kerkwijk, Breton & Kulkarni 2011).

### 2. OBSERVATIONS

Examination of plots of white light CCD photometry made on Oct. 31 and Nov. 1, 2010 with the 1m Lulin Telescope (Taiwan) and on November 11, 2010 with the 0.81m Tenagra Telescope (Arizona) allowed us to infer an orbital period of  $\sim 0.19$  d. The source appears in the SDSS DR8 data release with colors  $u=20.85$ ,  $g=19.00$ ,  $r=18.61$ ,  $i=18.25$ ,  $z=18.23$ , suggesting a G-type spectral class. Optical extinction at this high latitude is very small ( $A_V \approx 0.1$  from the Schlegel et al. 1998 dust maps). Based on the large ( $> 2.5$  mag) variation it seemed likely that this is a nearby, short-period black-widow type pulsar, with a strongly heated companion and thus a suitable target for detailed optical spectroscopy.

#### 2.1. HET, SSO and WIYN Photometry

The 9.2 m Hobby-Eberly Telescope (HET) has a spherical primary with a tracking corrector and can follow a source for  $\sim 1$  hr/night during a transit. This is a small fraction of the estimated 4.6 h orbital period. However the HET is dynamically queue scheduled (Shetrone et al. 2007), and with an ephemeris one can obtain full orbital coverage. During HET Low Resolution Spectrograph (LRS) observations one obtains short direct images for target acquisition. We used these 3–15 s ‘pre’ images, augmented by ‘post’ images in several cases, to monitor the flux of J2339–0533. These images, through a Schott GG385 long-pass filter, approximate the ‘white light’ of the 2010 photometry. We measured simple differential aperture magnitudes, calibrated to the SDSS  $r'$  magnitudes of nearby stars. These photometric data covering Aug. 5 through Sept. 6 2011 confirmed the dramatic optical modulation of J2339–0533. Conditions were variable, but detections were always of high S/N, even at the  $r' \sim 21$  minimum.

<sup>1</sup> Visiting Astronomer, Kitt Peak National Observatory, National Optical Astronomy Observatory, which is operated by the Association of Universities for Research in Astronomy (AURA) under cooperative agreement with the National Science Foundation. The WIYN Observatory is a joint facility of the University of Wisconsin-Madison, Indiana University, Yale University, and the National Optical Astronomy Observatory.

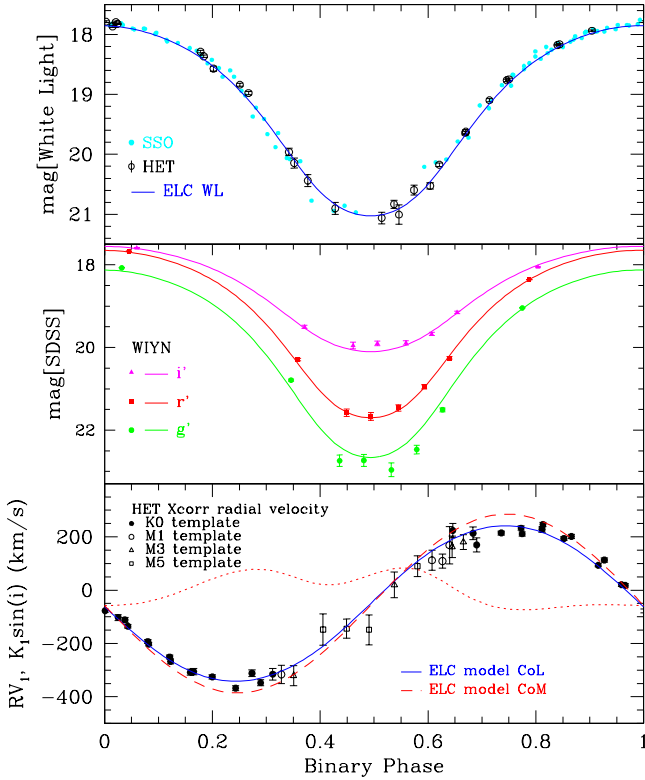


FIG. 1.— HET/SSO/WIYN measurements of J2339–0533. Upper panel: white light photometry (normalized to SDSS  $r$ ). The curve gives the best-fit ELC model fit. Middle panel: WIYN SDSS band color photometry and ELC models. Lower panel: radial velocity measurements. Symbols indicate the MK class of the best-fit cross-correlation template. Curves show the model radial velocity for the Center-of-Light (solid) and Center-of-Mass (dashed) from the ELC fit. The dotted line shows  $10\times$  the non-linear  $RV_1$  variation  $10(RV_1 - 0.9K_1\sin(i))$ .

Since the target is very bright, we obtained additional photometry with the 0.61 m Cassegrain telescope at the Stanford Student Observatory (SSO) on Aug. 28, 2011 (MJD 55801.287 – .399) and Oct. 20, 2011 (MJD 55855.140 – .381). Using 300 s unfiltered CCD exposures with an Apogee AP8 camera, we made differential flux measurements, again normalized to SDSS  $r'$  magnitudes. These data helped in absolute phasing and improving the binary period estimate.

Finally, we obtained SDSS  $g'r'i'$  frames at the 3.6 m WIYN telescope using the MiniMo camera on Sept. 27, 2011 (55832.290 – .424). These data, covering inferior conjunction, were used to constrain the color variation through minimum (inferior conjunction IC).

After converting exposure midpoint times to the solar system barycenter, we minimized residuals to obtain an accurate orbital period (Table 1, errors from bootstrap). The epoch (jointly fit with the radial velocity data, see below) defines superior conjunction (approximately maximum light). The photometric data folded at this period are shown in figure 1.

## 2.2. Archival X-ray Light Curve

We used this ephemeris to extract an X-ray light curve from the archival 21 ks *CXO* ACIS-I exposure of the 0FGL J2339.8–0530 field taken on Dec 13, 2009 (MJD 55117.54, obs 11791, T. Cheung PI), covering 1.25 orbits. Figure 2 shows the exposure-corrected light curve. The source is clearly modulated, with a relatively constant emission from phase -0.25 to 0.25, and a deep minimum at inferior conjunction (phase 0.5). The source is, however, detected at minimum.

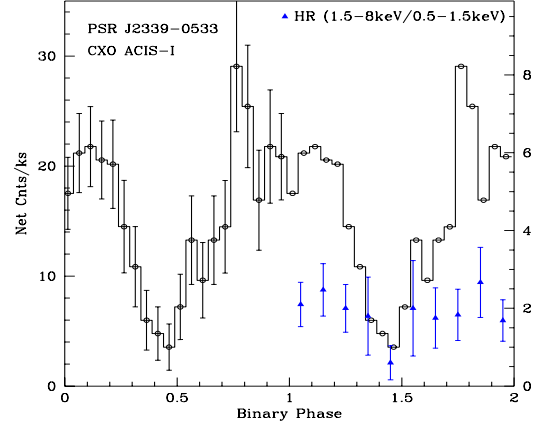


FIG. 2.— Two periods of the X-ray orbital light curve of J2339–0533. Statistical errors on the bin exposure-corrected count rate are shown during the first period. A simple 1.5–8 keV/0.5–1 keV hardness ratio is plotted (right scale) during the second period.

A simple absorbed power-law fit to the phase-averaged data gives a hard index  $\Gamma = 1.09^{+0.40}_{-0.13}$  and no significant absorption  $N_H < 1.6 \times 10^{21} \text{ cm}^2$  with a (0.5–8 keV) flux  $2.3^{+1.2}_{-0.3} \times 10^{-13} \text{ erg cm}^{-2} \text{ s}^{-1}$  (all 90% errors). Lacking counts for a phase-resolved spectral analysis, we can extract a simple hardness ratio. Intriguingly, this is lowest at  $\phi = 0.5$  (IC), suggesting that the hard spectrum source dominates near SC, but is deeply absorbed or eclipsed revealing a softer component at IC. Deeper X-ray observations are clearly needed to probe the orbital spectral variations.

## 2.3. Spectroscopy

For the spectroscopic exposures we used the HET LRS, employing grism 2, with a GG385 filter and a 1.5 arcsec slit. This covered  $\lambda\lambda 4283\text{--}7265\text{\AA}$ , at a resolution of  $1.99\text{\AA}/\text{pixel}$ , for an effective  $R \sim 1000 - 1200$ . All observations were taken with the slit at the parallactic angle and we limited exposures to 600 s to minimize velocity smearing to  $< 35 \text{ km/s}$ . The HET pupil varies as the corrector tracks across the primary, so significant changes in the PSF and hence in the line profile of stellar sources occurs at the extrema of the tracks. Since we are seeking maximal radial velocity accuracy, velocities from observations very early or late in a transit may be compromised. For most HET visits, we were able to obtain 3–4 600 s exposures; however a few exposures were taken far from the track center and were omitted from the orbital velocity fits. J2339–0533 lies relatively near the HET’s DEC =  $-11^\circ$  southern limit. It is thus possible to extend visit times by resetting the telescope azimuth during the exposure sequence. On Sept. 1, 2011, we obtained such a ‘long track’ re-setting the azimuth twice and allowing  $9 \times 600 \text{ s}$  exposure to be obtained (spanning  $\sim 2$  hours or 0.42 of orbital phase) with only modest tracker excursion. Thus, under favorable circumstances, the HET can obtain extended integrations during a single visit at the cost of queue efficiency. In total  $48 \times 600 \text{ s}$  exposure were obtained during one month of queue observations under variable conditions, equivalent to a full night of classical observation.

Data reduction was performed with the IRAF package (Tody 1986; Valdes 1986) using standard techniques. Biases, dome flats and arc lamp exposures were obtained nightly. All data were bias subtracted, and flat fields were applied after removal of the lamp response. Arc exposures were used for wavelength calibration. Checks of the sky lines showed that these solutions were stable to  $\sim 0.3\text{\AA}$  during a single visit

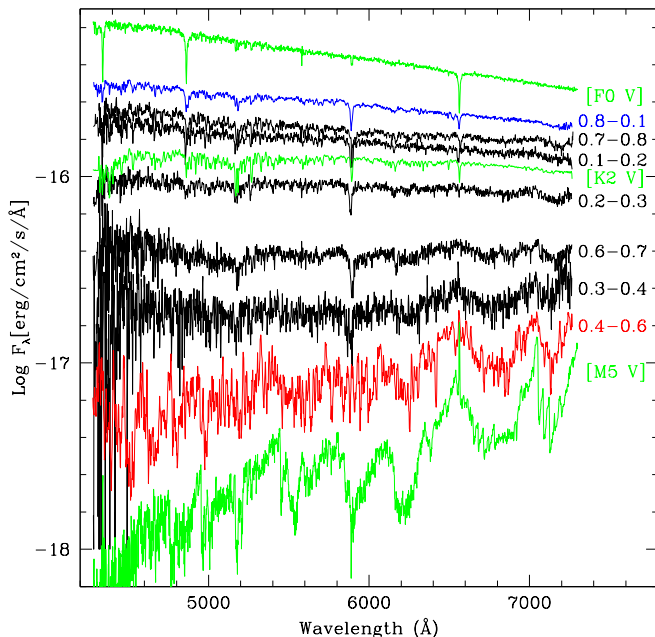


FIG. 3.— Averaged spectra for several phase bins during the orbit of J2339-0533. Green traces show three comparison spectra [F0,K2,M5]. The average of  $0.8 < \phi < 0.1$  at superior conjunction (maximum) shows an  $\sim$ F-type continuum, with weaker Balmer emission and stronger metal lines. The average of  $0.4 < \phi < 0.6$  at inferior conjunction (minimum) shows a M-type spectrum, dominated by the molecular complexes, but with some blue excess. Intermediate spectra represent phase ranges of 0.1 and are adequately traced by K-type spectra, trending toward M.

and  $\sim 0.7\text{\AA}$  night-to-night; sky lines were monitored to subtract out these residual shifts, leading to an estimated stability of  $0.1\text{\AA}$  for the wavelength scale. Spectra were optimally extracted (Valdes 1992) and visually cleaned of residual cosmic rays. Spectrophotometric calibration was performed using standard stars from Oke (1990) and Bohlin (2007). Occasionally appropriate standards were not measured during a given night; data from a neighboring queue night were then employed. The fluxing was not reliable for  $\sim 20\text{\AA}$  at the ends of the spectra and these were generally excluded from the final analysis. Spectra were corrected for atmospheric extinction using the KPNO extinction tables. Telluric templates were generated from the standard star observations in each night, with separate templates for the oxygen and water line complexes. We corrected separately for the telluric absorptions of these two species. We found that most telluric features divided out well, with significant residuals only apparent in spectra with the highest S/N.

The final cleaned, calibrated spectra were averaged to study the companion spectrum at various orbital phase bins (Figure 3). Although the LRS does not cover much of the far blue used for traditional MK classification, there are clear continuum and line dominance trends through the orbit. Comparison with the Gray on-line atlas<sup>1</sup> and with sample spectra from the SDSS DR8 SEGUE Spectroscopic Parameter Pipeline (SSPP)<sup>2</sup> (Lee, et al. 2008) allows reasonably accurate temperature classification. The spectrum evolves from a  $\sim 6900\text{ K}$  F3 type continuum at flux maximum to a  $\sim 2900\text{ K}$  M5 class spectrum near flux minimum. In general the bright phase spectra show stronger metal line absorptions than the corresponding continuum spectral class; Na I D at the stellar

TABLE 1  
J2339–5033 SYSTEM PARAMETERS

Parameter	ELC fit value
RA (J2000)	23:39:38.75
DEC (J2000)	-05:33:05.3
$P_b$ (d)	$0.19309790 \pm 1 \times 10^{-7}$
$T_0$ (MJD-TDB)	$55500.4833 \pm 0.0002$
$M_1 (M_\odot)$	$0.075 \pm 0.007$
$M_2 (M_\odot)$	$1.40 \pm 0.04$
$i$ (deg)	$57.4 \pm 0.5$
$f_1$	$0.90 \pm 0.01$
$T_1$ (K)	$2800 \pm 50$
$\log[L_X]$ (erg/s)	$33.5 \pm 0.1$

radial velocity is particularly strong at all phases away from inferior conjunction.

Velocity shifts of individual exposures were computed by cross correlation against dwarf star spectral templates (from the SDSS spectral library) using the IRAF rvsao package. Templates from F0 through M5 were used. We found that K0 templates provided the largest cross-correlation amplitude for most phases, despite continuum colors matching hotter spectral classes near maximum – we attribute this to the fact that the effective spectrum is composite.

Near phase 0.5 the spectrum is increasingly dominated by molecular bands and the best cross-correlations (and effective spectral class) move through M0 to M5. At these phases, the spectra are very red and improved correlation was often found when the data were trimmed by 500-1000Å in the blue. Even at flux minimum we obtained cross-correlation coefficients  $R > 3$ , except for a few poorly exposed spectra at large tracker offset (small effective telescope aperture). These were dropped from the radial velocity study. Typical correlations had  $R \sim 15 - 25$  and radial velocity errors 8-12 km/s. The radial velocity points and errors are shown in the bottom panel of Figure 1, with symbol type indicating the highest correlation spectral class.

### 3. BINARY SYSTEM PROPERTIES

Normally for pulsar binaries we have a precision mass function and orbital ephemeris from the radio arrival times, which greatly restrict the range of viable model solutions. However, even without a pulse detection, we can still use our HET/SSO/WIYN photometry and spectroscopy to place preliminary constraints on the orbital parameters of the J2339–0533 system, using the ELC code of Orosz & Hauschildt (2000). This code includes the effect of companion illumination ‘X-ray heating’ and estimates light curves based on the low temperature ‘NextGen’ atmosphere tables. A table adapted for SDSS filters and white light photometry was kindly generated by J. Orosz. As found by Reynolds, et al. (2007) for PSR B1957+20, the low  $T_{eff}$  atmospheres were essential to allowing the model to produce reasonable light curves; the black-body approximation produced models too bright at orbital minimum. For the fits we adjusted the companion unheated (backside) effective temperature  $T_1$  and Roche lobe fill factor  $f_1$ , the pulsar heating flux  $L_x$ , and the orbital semi-major axis  $a$ , mass ratio  $q$ , inclination  $i$  and phase of superior conjunction.

The best fit parameters (Table 1, light curve and radial velocity models in Figure 1) indicates a cool companion, intermediate inclination and moderate X-ray heating. This solution suggests a mass ratio  $q = 18.5 \pm 1$  and a relatively

<sup>1</sup> [http://nedwww.ipac.caltech.edu/level5/Gray/Gray\\_contents.html](http://nedwww.ipac.caltech.edu/level5/Gray/Gray_contents.html)

<sup>2</sup> <http://www.sdss3.org/dr8/spectro/sspp.php>

massive companion  $M_1 = 0.075 M_\odot$ . The errors quoted are statistical only. Figure 1 also shows the companion center-of-mass (CoM) velocity; note the substantial decrease in amplitude and small shape distortions of the center-of-light (CoL) curve. We caution that, with a reduced  $\chi^2 \approx 3$ , systematic errors are substantial and secondary fit minima are present.

Overall, the good agreement with the ‘black widow’ picture is encouraging. For all fits the models remain slightly too hot ( $g'$  too bright,  $i'$  too faint) at pulse minimum, suggesting amendments to the pass bands or the heating and albedo model are needed. Also the best fit epoch from the radial velocities alone shifts  $\delta\phi \sim 0.005(\delta T_0 = 0.001 \text{ d})$  from that of the full fit, implying that improvements in the spectral weighting could be helpful. Additional color photometry and especially a pulsar mass function and phase measurement should tighten up the fits considerably.

#### 4. CONCLUSIONS AND IMPLICATIONS

Our data also give some constraint on the distance and spin-down luminosity of the putative pulsar. At phase 0.25 the companion is half-illuminated, with  $T_{eff} \approx 4800 \pm 200 \text{ K}$ . Adopting the companion fit radius  $R_2 = 0.24 R_\odot$  and scaling from a main sequence star gives an expected  $M_r = 8.7 \pm 0.3$ . The observed  $m_r = 18.8 \pm 0.2$  then indicates a distance of  $1.1 \pm 0.3 \text{ kpc}$ . The *CXO* flux gives a pulsar X-ray luminosity of  $\approx 3 \times 10^{31} \text{ erg s}^{-1} d_{kpc}^2$ . This is substantially less than the  $3 \times 10^{33} \text{ erg s}^{-1}$  heating effect observed from the companion. Note, however that Becker (2009) has found that pulsars have  $L_X \approx 10^{-3} \dot{E}$  so that we would infer a spin-down luminosity of  $\sim 3 \times 10^{34} d^2 \text{ erg s}^{-1}$ . Thus, again like PSR B1957+20, we find that a substantial fraction  $\sim 0.1 - 0.3$  of the expected spindown luminosity goes into heating the companion. We can obtain an additional estimate of the pulsar spindown luminosity from the observed  $F_\gamma = 3 \times 10^{-11} \text{ erg s}^{-1}$ , since a heuristic  $\gamma$ -ray luminosity  $L_{\gamma,heu} \approx (\dot{E} \times 10^{33} \text{ erg/s})^{1/2}$  has been found for other  $\gamma$ -ray pulsars (Abdo et al. 2010), where  $L_\gamma = 4\pi f_\Omega F_\gamma d^2$  and  $f_\Omega$  should be in the range  $0.7 - 1.3$  Watters et al. (2009). This gives an estimate  $\dot{E} \approx 1.3 \times 10^{34} f_\Omega^2 d^4 \text{ erg s}^{-1}$ . All of these estimates support the identification with a  $\dot{E} \approx 2 \times 10^{34} \text{ erg s}^{-1}$  pulsar, somewhat less luminous and closer than PSR B1957+20, but consistent with the other BW-type pulsars recently discovered in the direction of *Fermi* sources (Roberts 2011).

We conclude that the  $\gamma$ -ray source is an energetic pulsar evaporating a low mass companion. Our preliminary photometry and model fits suggest a somewhat larger companion mass than for the original black widow pulsar PSR B1957+20. Our present estimate of  $i \sim 57^\circ$  implies that we should not see a  $\gamma$ -ray eclipse. However the substantial drop of the X-

ray flux at phase 0.3–0.6 suggests a strong wind absorbing much of the X-ray emission.

To date no  $\gamma$ -ray millisecond pulsar has been discovered in a blind search of the LAT photons, since the  $\sim \text{ms}$  periods require many trials in pulsar spin frequency and position space. Since most MSP are in binaries the additional trials needed to cover binary acceleration makes the searches prohibitively expensive. One of our prime motivations in this project has been to reduce the binary phase space of trials needed to search J2339–0533 and enable such a discovery. Our data tightly constrain the period and phase of the pulsar reflex motion and suggest an amplitude  $a_2 \sin i \approx 0.16 \text{ lt-s}$ . These constraints are insufficient for a direct fold, but greatly restrict the number of binary trials needed.

If a  $\gamma$ -ray (or radio) pulse detection is made, this system provides an excellent opportunity for study of the pulsar mass and binary evolution. The resulting precise mass ratio  $q$  will restrict the fit space, improving mass estimates for PSR J2339–0533 and its companion. Further optical and X-ray spectroscopy of this bright system can measure the surface heating in more detail and probe the density of the evaporative wind. If highly eclipsed radio emission is discovered, this suggests radio beams closely coincident with the  $\gamma$ -ray emission. Conversely, if no pulsed radio emission is found while viewing at relatively clear orbital phases and folding at a known pulsar period, this could represent the first truly ‘radio-quiet’ millisecond pulsar. As it is, we have built such a strong circumstantial case that it is fair to refer to J2339–0533 as a probable millisecond pulsar; all we are missing is the spin period itself.

We wish to thank Albert Kong for drawing our attention to recent progress on identifying the counterpart and for sharing plots of the Lulin optical photometry. Jerome Orosz and Jeff Coughlin kindly supplied copies of the ELC code. We also particularly wish to thank the Hobby\*Eberly Telescope RA team of Matthew Shetrone, John Caldwell, Steve Odewan and Sergiy Rostopchin, for their excellent efforts in obtaining good orbital phase coverage of this short-period binary.

This work was supported in part by NASA grants NNX10AD11G and NNX11AO44G.

The Hobby\*Eberly Telescope (HET) is a joint project of the University of Texas at Austin, the Pennsylvania State University, Stanford University, Ludwig-Maximilians-Universitaet Muenchen, and Georg-August-Universitaet Goettingen. The HET is named in honor of its principal benefactors, William P. Hobby and Robert E. Eberly. The Marcario Low Resolution Spectrograph is named for Mike Marcario of High Lonesome Optics, who fabricated several optics for the instrument but died before its completion. The LRS is a joint project of the Hobby\*Eberly Telescope partnership and the Instituto de Astronomia de la Universidad Nacional Autonoma de Mexico.

#### REFERENCES

- Abdo, A.A. et al. 2009a, *ApJS*, 183, 46
- Abdo, A.A. et al. 2009b, *Science*, 325, 840
- Abdo, A.A. et al. 2010, *ApJS*, 187, 460.
- Abdo, A.A. et al. 2011, *ApJS*, submitted
- Ackerman, M. et al. 2011, *ApJ*, submitted
- Archibald, A. et al. 2010, *ApJ*, 722, 88.
- Becker, W. 2009, *ASSL*, 357, 91
- Bohlin, R. C. 2007, *ASPconf*, 364, 315
- Kong, A. et al. 2011a, *AAS*, 218, 32005.
- Kong, A. et al. 2011b, *ApJ*, in prep.
- Lee, Y.S., et. al 2008, *AJ*, 136, 2022
- Oke, J. B. . 1990, *AJ*, 99, 1621
- Orosz, J.A. & Hauschildt, P.H. 2000, *AA*, 364, 265
- Roberts, M.S.E. 2011, *AIP Conf.*, 1357, 127
- Reynolds, M.T. et al. 2007, *MNRAS*, 379, 1117
- Schlegel, D. J., Finkbeiner, D. P. & Davis, M. 1998, *ApJ*, 500, 525.
- Shetrone, M. et al. 2007, *PASP*, 119, 556
- Tam, P.H.T. et al. 2010, *ApJ*, 724, 207
- Tody, D. 1986, *SPIE*, 627, 733
- Valdes, F. 1986, *SPIE*, 627, 749
- Valdes, F. 1992, *ASPconf*, 25, 417
- van Kerkwijk, M.H., Breton, R.P. & Kulkarni, S.R. 2011, *ApJ*, 728, 95.

Watters, K.P. et al. 2009, *ApJ*, 695, 1289